Supplementary Information (SI) for ChemComm.
This journal is © The Royal Society of Chemistry 2025

Electronic Supplementary Information

From micro-to-nano in charged water microdroplets: Unveiling steps in the weathering of minerals †

Anubhav Mahapatra,[a] Anirban Som,[a] B. K. Spoorthi,[a] Depanjan Sarkar,[a c] and Thalappil Pradeep *[a b c]

[a.]DST Unit of Nanoscience (DST UNS) & Thematic Unit of Excellence (TUE), Department of Chemistry, Indian Institute of Technology Madras (IITM), Chennai - 600036, India.

[b.]International Centre for Clean Water, 2nd Floor, B-Block, IIT Madras Research Park, Kanagam Road, Taramani, Chennai - 600113, India.

[c.]Centre of Excellence on Molecular Materials and Functions, Department of Chemistry, Indian Institute of Technology Madras, Chennai – 600036, India.

Table of contents

S1. Materials:

River sand and natural ruby samples were procured from a local marketplace and used without further purification. The samples were mechanically ground using mortar and pestle to obtain fine powders. Ultrapure milli-Q water (18.5 MΩ·cm at 25 °C) was employed throughout the experimental procedures. The resulting ground materials were then dispersed in milli-Q water to form particle suspensions. These suspensions were subjected to ultrasonication using an ultrasonic bath having specifications 40 kHz, 100 W for 10 minutes to enhance dispersion and break up agglomerates. Subsequently, the suspensions were centrifuged with Remi RM-03 Plus for 1 minute to achieve preliminary size separation, allowing the removal of larger particulates and enrichment of finer and mid ranged micro-particles.

S2. Electrospray deposition experiments:

A custom-built electrospray setup as shown in Fig. 1 was used to generate microdroplets. The use of gastight Hamilton syringe (0.5 mL) with 22 gauge (inner diameter of 413 µm) needle was connected with 50 µm inner diameter fused silica capillary via union connector. The syringe needle was connected with the high voltage power supply and the carbon coated copper TEM grid with 300 mesh was kept on the plate collector and it was grounded. The stepper motor with 400 steps per rotation was used to control the flow rate of the suspension precisely. The deposition experiments were conducted in ambient conditions of 25 °C and relative humidity of 50-60 % for 1 hour. Polyimide coated fused silica capillary was procured from Polymicro Technologies™, Molex, USA and the other components like union connector, PEEK tubing, ferrules were purchased from IDEX Health & Science, USA.

S3. Characterization:

Thermo Fisher Scientific Verios G4 UC high-resolution field emission scanning electron microscope (FESEM) at an accelerating voltage of 10 kV with emission current of 0.10 nA was used to image the micro-sized particles of quartz and ruby. A thin layer of gold ~ 0.2 nm was sputtered on the sample kept on aluminium substrate by use of Quorum Q150T S plus to make it conductive and necessary for FESEM imaging. Glow discharge was used for carbon coated copper TEM grids to remove unnecessary impurities and make the surface more hydrophilic by Quorum GloQube Plus and Thermofischer Talos™ F200i transmission electron microscope (TEM) was used at an accelerating voltage of 200 kV to image the nanoscale particles of quartz and ruby.

S4. Nebulization of quartz and ruby suspension:

Suspensions of quartz and ruby (0.2 mg/mL) were prepared according to the method detailed in Section S1. These were separately loaded into a Hamilton syringe and dispensed through a polyimide-coated fused silica capillary (50 µm inner diameter) using a syringe pump. Nitrogen gas (N_2) at 50 psi was used to nebulize the suspension and generate microdroplets. No applied potential was used, ensuring that the generated droplets remained largely uncharged. The capillary was directed into a 100 mL round-bottom flask to collect the products over 30 minutes, after which the collected materials were redispersed in ultrapure water. 20 µL aliquot

of the collected suspensions were drop-cast onto carbon-coated TEM grids and allowed to dry. As shown in the TEM images in Fig. S5, the disintegration of mineral particles into nanoparticles was not feasible with neutral microdroplets, which resulted in the formation of larger aggregates of particles.

S5: Mechanical factors influencing the fragmentation of mineral particles:

The distinct fragmentation behaviors of minerals in charged water microdroplets can be attributed to their hardness and elastic moduli. Ruby, characterized by strong Al–O bonds and dense atomic packing, has a high elastic modulus (~ 400 GPa) and high hardness. In contrast, quartz exhibits a lower elastic modulus (~117 GPa).[1,2] These properties hinder slippage of lattice planes in ruby, delaying initiation of fragmentation compared to quartz. Consequently, the combined influence of high hardness, elevated elastic modulus, and concentrated charges at the droplet interface necessitates higher potentials for the fragmentation of ruby.

Supplementary figures:

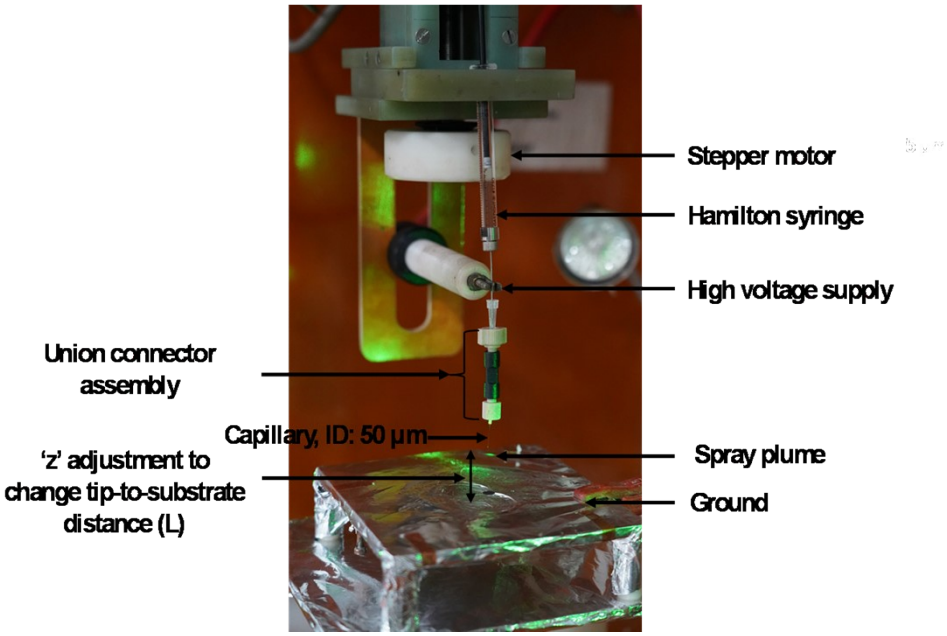

Fig. S1: Photograph of the device used for electrospraying. A TEM grid was kept on the substrate below the tip of the capillary at different tip-to-substrate distances. The spray plume was illuminated by a green laser.

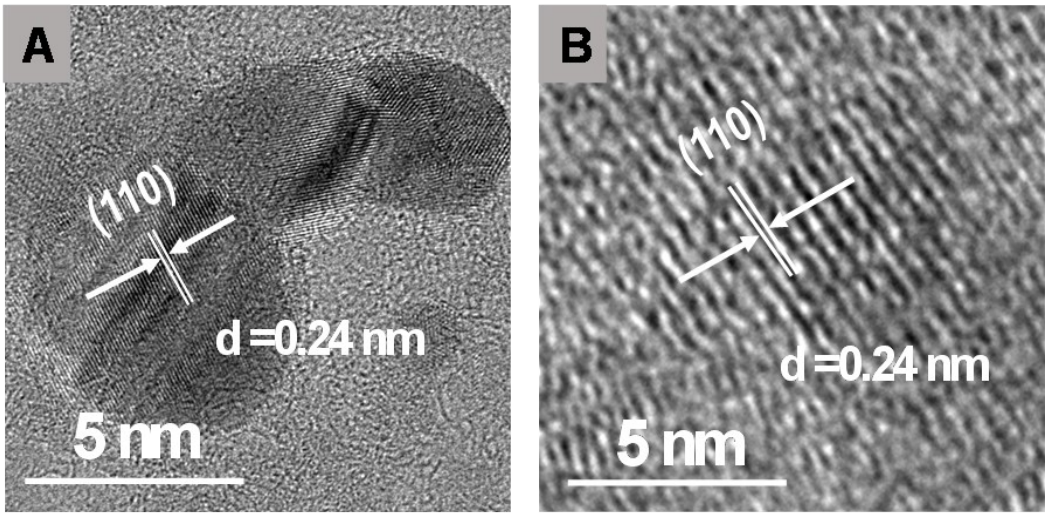

Fig. S2: High-resolution transmission electron microscopic (HRTEM) images showing the plane (110) of quartz in **A)** disintegrated intermediate species and **B)** nanoparticle.

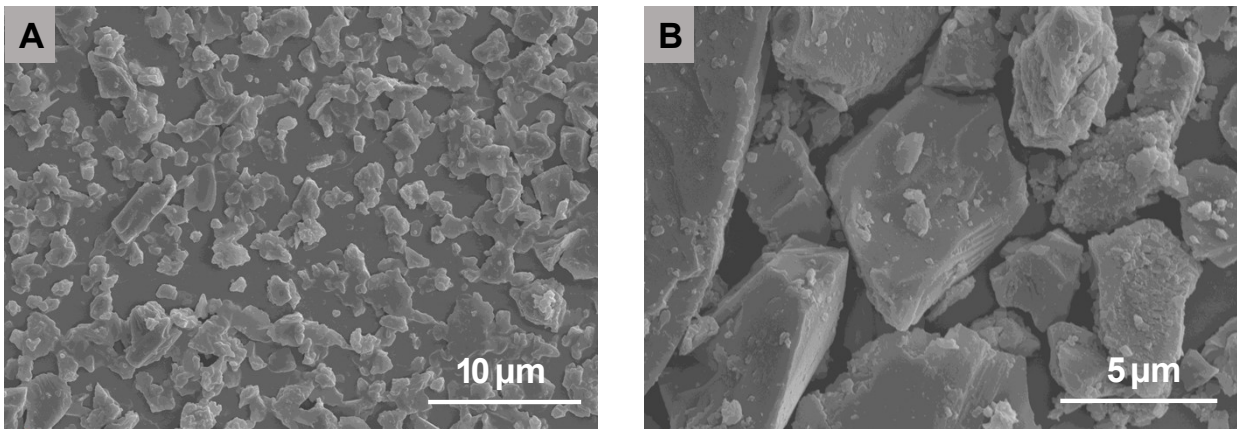

Fig. S3: Field emission scanning electron microscopic (FESEM) images of ruby particles before electrospray at different scale bar **A)** 10 µm and **B)** 5 µm**.**

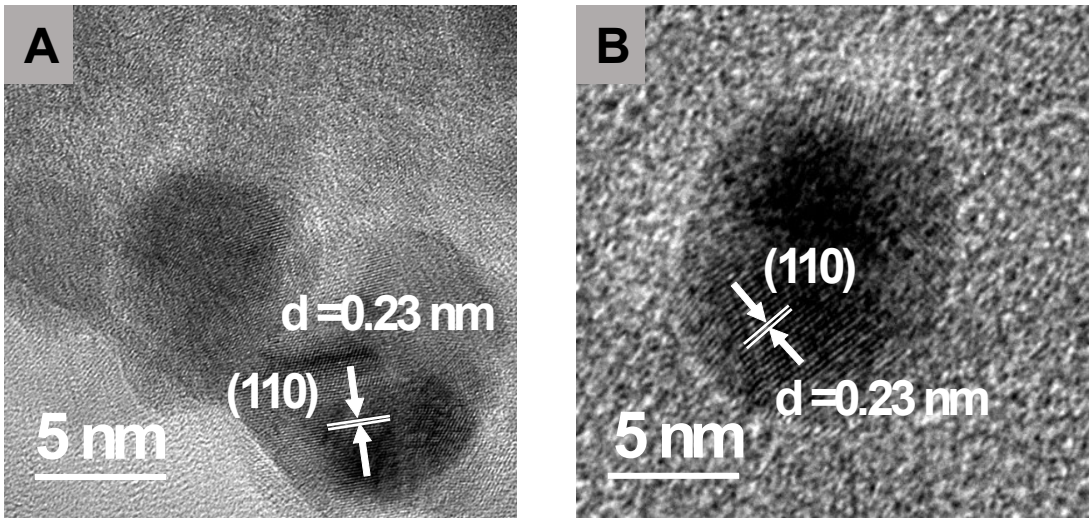

Fig. S4: High-resolution transmission electron microscopic (HRTEM) images showing the plane (110) of ruby in **A)** disintegrated intermediate species and **B)** nanoparticle.

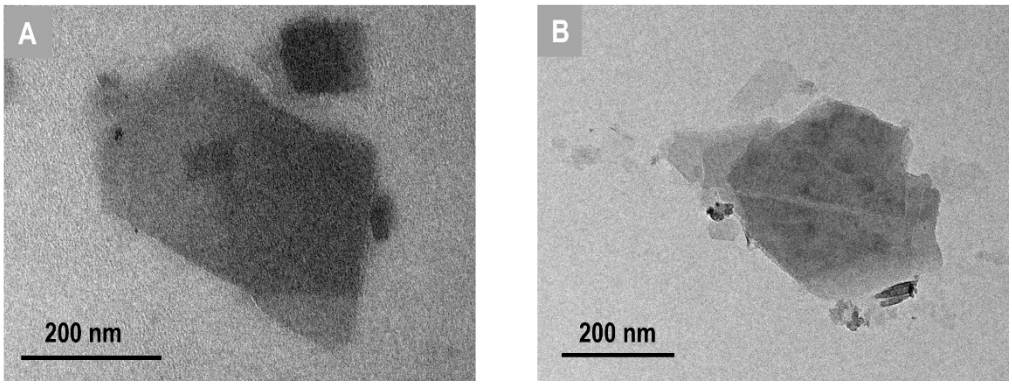

Fig. S5: TEM images showing bigger aggregates of **A)** quartz and **B)** ruby upon nebulization with N_2 at a pressure of 50 psi.

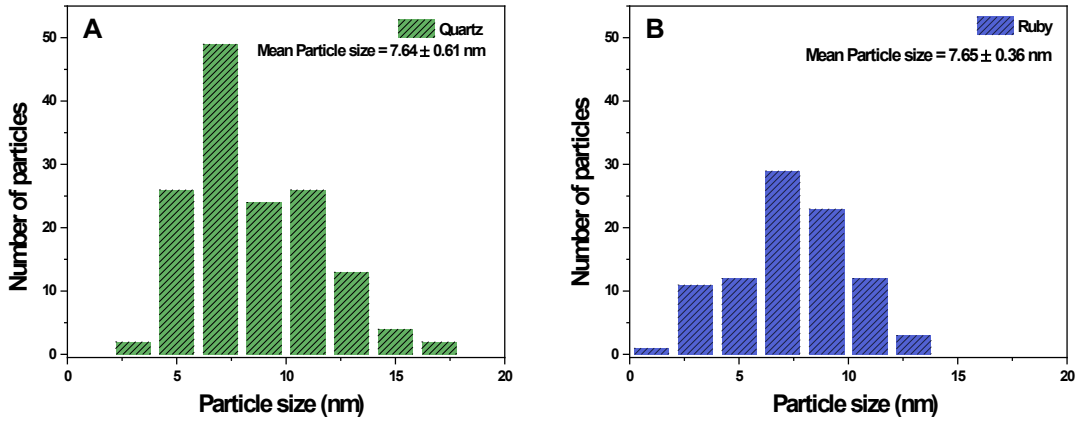

Fig. S6: Particle size distribution of nanoparticles of **A)** quartz and **B)** ruby.

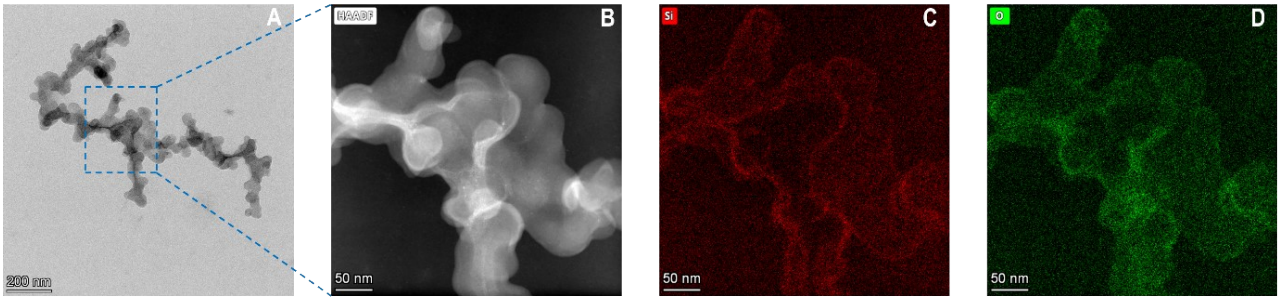

Fig. S7: Flower-like intermediate species of quartz **A)** TEM image; **B)** HAADF image of the magnified portion of the image; EDS elemental mapping showing the presence of **C)** Silicon and **D)** Oxygen.

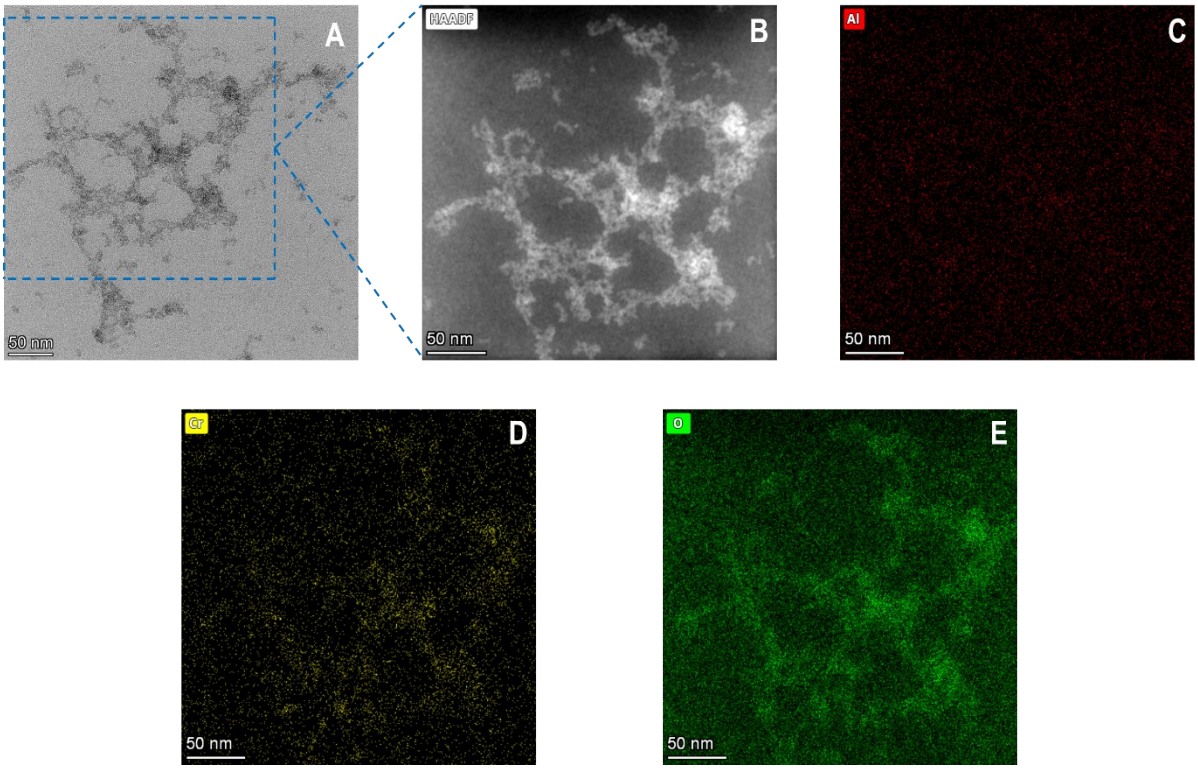

Fig. S8: Flower-like intermediate species of ruby **A)** TEM image; **B)** HAADF image of the magnified portion of the image; EDS elemental mapping showing the presence of **C)** Aluminium; **D)** Chromium; and **E)** Oxygen.

References:

1 L. Zhang, F. Jiao, W. Qin and Q. Wei, *ACS Omega*, 2023, **8**, 43644–43650.

2 S. Ruppi, A. Larsson and A. Flink, *Thin Solid Films*, 2008, **516**, 5959–5966.